NASA Technical Memorandum 83801

The Effect of Channel Convergence on Heat Transfer in a Passage With Short Pin Fins

Barbara A. Brigham
Lewis Research Center
Cleveland, Ohio

October 1984

NASA

THE EFFECT OF CHANNEL CONVERGENCE ON HEAT TRANSFER

IN A PASSAGE WITH SHORT PIN FINS

Barbara A. Brigham
National Aeronautics and Space Administration
Lewis Research Center
Cleveland, Ohio 44135

E-2306

SUMMARY

Results from a series of experiments are presented showing the effect of channel convergence on heat transfer in short pin fins as used in turbine blade internal cooling schemes. Array averaged heat transfer coefficients were obtained for two configurations of staggered arrays of short pin fins in a converging channel. One configuration contained pins with length to diameter ratio of two in a constant height channel with channel sidewalls converging to give an area ratio of two to one from inlet to outlet, giving only accelerated flow. The second configuration contained pins in a constant width channel with the top and bottom surfaces of the channel converging and with length to diameter ratio varying from two to one streamwise through the test section. This configuration had the same area ratio from inlet to outlet as in the first configuration, giving varying pin length as well as accelerated flow. In addition to the pin fin configurations, two flat plate configurations were also tested which had the same geometries as the pin fin configurations but no pins.

Results show that for the constant height pin fin configuration, the Nusselt numbers are approximately the same as in previous tests done on straight channel test sections with pins of the same length to diameter ratio. For the constant width pin fin configuration, results indicate Nusselt numbers approximately 20 percent lower than for tests performed on configurations with constant pin length in the same range of length to diameter ratio. This suggests that the varying pin length does have some effect on the heat transfer, but that the flow acceleration has a negligible effect. For the flat plate configurations, both indicate Nusselt numbers in the same range as is other similar flat plate tests. As in the above mentioned pin fin tests, the constant width configuration exhibited Nusselt numbers slightly lower (about 6 percent) than for the constant height configuration. This shows that a constant width configuration (pin fin or flat plate) exhibits a lower Nusselt number level than a constant height configuration.

INTRODUCTION

In modern gas turbine engines, there are many different types of turbine blade cooling schemes available to the designer. The method of particular interest in the present study is the use of short pin fins as used in trailing edge cooling passages. Until quite recently, the only information of this type available in the literature was for relatively long pins of more than four diameters in length. Since the length of the pin fins used for gas turbine applications is generally less than four diameters, most of this information could not be used effectively.

Recently, some data specifically for applications of pin fins to gas tur-
bines have become available. One program undertaken at Arizona State
University (refs. 1 to 3) measured the heat transfer from short pin fins ar-
ranged in staggered 10-row (streamwise) arrays. This work (refs. 1 and 2)
measured the spanwise-averaged heat transfer for both the pin and endwall sur-
faces on a row by row basis for pins with L_p/D of one. These results
showed that the heat transfer increased in the first four rows of the array
and then decreased slightly through the rest of the array. This was similar
to the trends found in long cylinder and tube bank data.

VanFossen (ref. 4) measured the heat transfer from both pin and endwall
surfaces for several staggered four-row (streamwise) arrays of short pin fins
with L_p/D of one half and two. It was found that for this range of length
to diameter ratio, all the data could be represented by a single curve. It
was also found that the heat transfer coefficients on the pin fin surface were
about 35 percent higher than on the endwall surface.

Another set of experiments determined the effect of position within an
array on the heat transfer to a single pin with L_p/D of three (ref. 5).
The results here indicated that the heat transfer to a single pin in a stag-
gered array increased significantly for one, two or three rows of pins added
upstream of the test pin. For four or more rows added upstream, the heat
transfer decreased slightly. This trend is similar to that found in refer-
ences 1 and 2. It was also determined that the average channel velocity
should be used as the reference velocity in the Reynolds number.

In reference 6 the effect of the number of rows and the length to diameter
ratio on the heat transfer was investigated. It was determined that the number
of streamwise rows has only a slight effect on the heat transfer to short pin
fins. The dominant effect, however, was the length to diameter ratio, with
L_p/D of four giving much higher heat transfer than was found in references
1, 2 and 4 for shorter pins. Reference 6 also showed that by using the average
channel velocity and the proper definition of the characteristic length, the
data of references 1 and 2 could be made to fall on the correlation derived in
reference 4.

Reference 7 presents heat transfer results for several short pin fin con-
figurations in which the length to diameter ratio varied streamwise through
the length of the test section. However, this work does not specifically ad-
dress the current objective and left unresolved which effect was dominant,
channel convergence with the resulting accelerating flow or varying length to
diameter ratio.

This paper presents the results of a series of tests designed to separate
the effects of varying pin length from channel convergence. Four test sections
were fabricated to give an area ratio from inlet to outlet of two to one. One
test section contained pins in a constant height channel with length to diame-
ter ratio of two with the channel sidewalls converging. Another test section
contained pins in a constant width channel with the top and bottom channel
surfaces converging and with length to diameter ratio varying from two to one
streamwise through the test section. The pins were all spaced 4 diameters
apart in an equilateral triangular array with four rows in the streamwise di-
rection, as in previous work done at NASA (refs. 4 and 6). Two other test
sections were fabricated which were identical to the above two test sections

2

but contained only flat plate surfaces (no pin fins). Heat transfer results are presented in the form of Nusselt number versus Reynolds number over a range of Reynolds numbers of interest for this application. Results are compared to those of references 4 and 6.

NOMENCLATURE

A'	average flow area, V/L, cm^2 $(in.^2)$
A_h	surface area of heaters, $2LW$, cm^2 $(in.^2)$
A_p	pin cross sectional area, $\pi D_0^2/4$, cm^2 $(in.^2)$
A_w	endwall area per pin, $(\sqrt{3}/2)(X_t D_0)^2$, cm^2 $(in.^2)$
D'	characteristic length, cm $(in.)$
D_0	pin diameter, cm $(in.)$
h'	average heat transfer coefficient in pin fin test section, $W/m^2 \cdot K$ $(Btu/hr \cdot ft^2 \cdot °R)$
h_{eff}	effective heat transfer coefficient, $W/m^2 \cdot K$ $(Btu/hr \cdot ft^2 \cdot °R)$
h_p'	average heat transfer coefficient on pin surface, $W/m^2 \cdot K$ $(Btu/hr \cdot ft^2 \cdot °R)$
h_w'	average heat transfer coefficient on endwall surface, $W/m^2 \cdot K$ $(Btu/hr \cdot ft^2 \cdot °R)$
k_a	thermal conductivity of air, $W/m \cdot K$ $(Btu/hr \cdot ft \cdot °R)$
k_p	thermal conductivity of pin material, $W/m \cdot K$ $(Btu/hr \cdot ft \cdot °R)$
L	test section streamwise length, cm $(in.)$
L_p/D	pin length to diameter ratio
1	pin half length, cm $(in.)$
m	fin parameter, $\sqrt{h'P/k_p A_p}$
Nu	Nusselt number, $h'D'/k_a$
P	pin perimeter, πD_0, cm $(in.)$
Q	heat dissipated in electric heater, W (Btu/hr)
Re	Reynolds number, $(w/A')D'/\mu$
S	total heat transfer surface area, cm^2 $(in.^2)$
T_{aw}	adiabatic wall temperature, K $(°R)$
T_r	Eckert reference temperature, K $(°R)$
T_s	static temperature, K $(°R)$
T_w	endwall temperature, K $(°R)$
V	flow channel volume minus pin volume, cm^3 $(in.^3)$
W	test section width, cm $(in.)$
w	mass flow rate, kg/s (lbm/s)

X_s ratio of pin height to pin diameter, (same as L_p/D)

X_t ratio of pin spacing to pin diameter, transverse direction

μ viscosity of air, kg/m·s (lbm/ft·s)

DESCRIPTION OF EXPERIMENT

Test Section and Flow Apparatus

A schematic of the rig used for the pin fin experiments is shown in figure 1. Room air was drawn through a constant acceleration inlet, into the test section and then through either an orifice flow meter (large flow rates) or through a venturi flow meter (small flow rates). The air passed through the respective flow control valves and then on into the laboratory altitude exhaust system. Air temperatures were measured at the test section inlet, test section outlet, and flow meters. Air density at the flow meters was calculated using the ideal gas law. The data were collected and converted to engineering units using the laboratory data collection system (ref. 8).

Figure 2 shows the test section assembly used for all the pin fin experiments. Shown in the figure are the inlet, endwall, and outlet thermocouples. The top and bottom surfaces of the inlet were covered with fine grit sandpaper and a 0.519 cm (0.063 in.) diameter trip wire was attached to the surface in order to ensure turbulent flow. The test section was enclosed in cloth-reinforced phenolic plastic and the entire assembly was wrapped in fiberglass insulation in order to minimize heat losses.

Figures 3 and 4 show schematics of the two pin fin test sections used, illustrating the channel geometry. Figures 5 and 6 show the assembled pin fin test sections, viewed in the direction of flow. These pictures show the difference in the convergence between the constant height configuration and the constant width configuration. The two flat plate test sections were identical in geometry but have no pin fins. Each test section was made of two 0.635 cm (0.250 in.) thick copper plates, with holes drilled for the insertion of the pins for the two pin fin test sections. The pins, which extended completely through the endwall plates, were soldered into place. The dimensions of the flow channels for all configurations are given in table I.

The test sections were heated with commercially available electric foil resistance heaters attached externally to the endwalls with pressure sensitive adhesive. The streamwise centerline temperatures of the endwalls were measured by thermocouples inserted into holes drilled along the edge of each endwall plate. The thermocouple connections and the electric heaters can be seen in figures 5 and 6.

Test Procedure

In order to account for heat losses, a set of calibrations was made for each test section with no air flow through the test section. By measuring the endwall temperatures, the ambient air temperature, and the total heat flux, an overall heat loss coefficient was determined for each configuration. This was done after the test section had reached a steady state condition, which was

usually overnight. During a data run, the Reynolds number was changed by varying the flow rate through the test section. The temperature of the endwall plates was kept constant using an electronic heater controlling system which regulated the power to each set of heaters.

Data Analysis

The theoretical model used as the basis for the pin fin data analysis is shown in figure 7. The total heat flux for the pin and endwall surfaces is the sum of the heat flux through the endwall and the heat flux through the pin. The average heat transfer coefficients on the pin surface and endwall surface are h_p' and h_w' respectively. The heat lost by the pin fin surface (endwalls included) is equated to the heat lost by a plain surface with heat transfer coefficient h_{eff}. For the purpose of this work, the average heat transfer coefficient on the pin, h_p', is assumed equal to the heat transfer coefficient on the endwalls, h_w', and is denoted by h'.

The overall loss heat transfer coefficient, h_{loss}, is defined as

$$h_{loss} = \frac{Q_{loss}}{A_h(T_w - T_a)} \tag{1}$$

This loss coefficient was found over a range of temperature differences, $T_w - T_a$, and a least squares curve fit was applied to the data with temperature as the independent variable. Thus, for a given temperature difference a corresponding loss coefficient could be found and the heat loss from the test section could be calculated.

The effective heat transfer coefficient, h_{eff}, is defined as

$$h_{eff} = \frac{(Q - Q_{loss})}{A_w(T_w - T_{aw})} \tag{2}$$

where T_{aw} is the adiabatic wall temperature calculated from

$$T_{aw} = T_s + r(T_t - T_s) \tag{3}$$

with r, the recovery factor, taken as the square root of the Prandtl number. The total temperatures were found by making an energy balance through the channel. The static temperatures were found using the compressible gas relationship between total and static temperatures.

Equation 2 gives the effective heat transfer coefficient, including the effects of pin efficiency. This can be rewritten as

$$Q_{total} = h_{eff}A_w(T_w - T_{aw}) \tag{4}$$

The heat flux through the endwalls is given by

$$Q_{wall} = h'(A_w - A_p)(T_w - T_{aw}) \tag{5}$$

5

where A_w is the endwall area and A_p is the cross-sectional area of the pin. The heat flux through the pin only is given by

$$Q_{pin} = \sqrt{Ph'k_p A_p}\tanh(ml)(T_w - T_{aw}) \tag{6}$$

with P being the perimeter of a pin, l being the half length of the pin, and the fin parameter m being defined by

$$m = \sqrt{\frac{h'P}{k_p A_p}} \tag{7}$$

The pin conductivity, k_p, was taken as 3.46 W/cm·K (200 Btu/hr·ft·°R). Then the energy balance yields the following equation:

$$h'\left(1 - \frac{A_p}{A_w}\right) + \left(\frac{\sqrt{Ph'k_p A_c}}{A_w}\right)\tanh(ml) - h_{eff} = 0 \tag{8}$$

The above transcendental equation was solved iteratively for h' for each measured value of h_{eff}.

For the flat plate test sections, an overall loss heat transfer coefficient was found as described above. Then since there were no pins, there was no need for an iterative procedure to solve for h'. The heat transfer coefficient is calculated as

$$h' = \frac{\left(Q - Q_{loss}\right)}{A_w(T_w - T_{aw})} \tag{9}$$

with h' being the average heat transfer coefficient on the endwall and sidewall surfaces in the plain channel.

The data was put in dimensionless form of Reynolds number and Nusselt number for purposes of comparison. The Reynolds number is defined as

$$Re = \left(\frac{w}{A'}\right)\frac{D'}{\mu} \tag{10}$$

where

$$D' = \frac{4V}{S} \tag{11}$$

$$A' = \frac{V}{L} \tag{12}$$

and μ is the viscosity of air. The Nusselt number is defined as

$$Nu = \frac{h'D'}{k_a} \tag{13}$$

where k_a is the thermal conductivity of air. Both μ and k_a were found from curve fits of data from reference 9 and were evaluated at the Eckert reference temperature (ref. 10), defined as

6

$$T_r = 0.5T_w + 0.28T_s + 0.22T_{aw} \tag{14}$$

The experimental uncertainty based on the method of Kline and McClintock (ref. 11) is less than three percent for the Reynolds number and less than four percent for the Nusselt number.

RESULTS AND DISCUSSION

Array averaged heat transfer coefficients for both pin and endwall surfaces were found for a range of flow rates and are presented in the form of Nusselt number versus Reynolds number for two pin fin configurations and two flat plate configurations in a converging channel. Figure 8 is a comparison of the constant height pin fin data with the results of references 4 and 6. The constant height data with L_p/D of two exhibits approximately the same Nusselt numbers as the correlation derived in reference 4 for L_p/D of less than or equal to two. In addition, the constant height data with L_p/D of two falls approximately 20 percent below both the four and eight row data of reference 6 with L_p/D of four. This difference is to be expected based on the results of reference 6. The effect of the channel convergence on the heat transfer to short pin fins of constant length to diameter ratio is merely a slight change in the slope of the data and virtually no change in the Nusselt number levels.

Figure 9 shows both the constant height data and the constant width data plotted with the correlation from reference 4. This correlation is for all short pin fins with length to diameter ratio between one half and two. It can be seen from figure 9 that the constant width data with L_p/D of two to L_p/D of one (the same range as in reference 4) fall approximately 20 percent below the correlation from reference 4. This is significant since the length to diameter ratios for these two sets of data are in the same range. One would have expected these two sets of data to be identical since the L_p/D are in the same range. Thus the changing pin length must be a significant factor. A least squares curve fit of the constant width data is

$$Nu = 0.147 \, Re^{0.667} \tag{15}$$

where the Nusselt number and Reynolds number are based on the characteristic length D'. Since the area ratios in both converging pin fin configurations are the same (two to one from inlet to outlet), it is apparent that in the constant width configuration the changing pin length has a significant effect on the Nusselt number level.

Figure 10 shows the current pin fin data and the current flat plate data plotted with the results of reference 4. It can be seen that both the constant height and the constant width flat plate data fall at approximately the same level as the nonconverging flat plate data from reference 4. This tends to indicate that these results are not rig dependent since the data from reference 4 were obtained in the same experimental facility. This also shows that there is not much effect on Nusselt number levels in converging configurations without pin fins. Also, the basic trend of the two sets of data are the same with the constant height configurations having consistently higher Nusselt number levels than the constant width configurations. This would tend to indicate that there may be some effect due to the direction of the convergence,

7

but this was not investigated in this program. Any further attempt to explain the reasons for the specific heat transfer characteristics in greater detail would necessitate a much more in-depth study of the flow field as well as measurements of the local pin and endwall heat transfer.

SUMMARY OF CONCLUSIONS

The results of this investigation of the effect of channel convergence on the heat transfer in short pin fins are as follows:

1. The constant height data with L_p/D of two exhibited Nusselt number levels approximately the same as the correlation derived by VanFossen, with a slightly different slope, however. Since the L_p/D is in the same range as the correlation of VanFossen, the effect of flow acceleration due to channel convergence in cases of constant L_p/D is negligible.

2. The constant width data with L_p/D of two to L_p/D of one falls approximately 20 percent lower than the correlation derived by VanFossen for the same range of L_p/D. It appears that the varying pin length has a definite effect on the heat transfer characteristics.

3. For tests on similar converging configurations using flat plates only (no pin fins), the flat plate data seems to have the same general behavior as nonconverging flat plates. This indicates no rig dependent behavior in the data.

4. The constant height configurations (both pin fin and flat plate) fall consistently higher than the constant width configurations. Therefore, there may be some effect due to the direction of the convergence. However, this effect was not investigated in the present program.

REFERENCES

1. Metzger, D. E.; Berry, R. A.; and Bronson, J. P.: Developing Heat Transfer in Rectangular Ducts with Arrays of Short Pin Fins. ASME Paper 81-WA/HT-6, Nov. 1981.

2. Metzger, D. E.; and Haley, S. W.: Heat Transfer Experiments and Flow Visualization for Arrays of Short Pin Fins. ASME Paper 82-GT-138, Apr. 1982.

3. Metzger, D. E.; Fan, Z. X.; and Shepard, W. B.: Pressure Loss and Heat Transfer Through Multiple Rows of Short Pin Fins. Heat Transfer 1982, vol. 3, U. Grigull, et al., eds., Hemisphere Publishing Corp., 1982, pp. 137-142.

4. VanFossen, G. J.: Heat Transfer Coefficients for Staggered Arrays of Short Pin Fins. J. Eng. Power, vol. 104, no. 2, Apr. 1982, pp. 268-274.

5. Simoneau, R. J.; and VanFossen, G. J.: Effect of Location in an Array on Heat Transfer to a Cylinder in Crossflow. J. Heat Transfer, vol. 106, no. 2, Feb. 1984, pp. 42-48.

6. Brigham, B. A.; and VanFossen, G. J.: Length to Diameter Ratio and Row Number Effects in Short Pin Fin Heat Transfer. J. Eng. Gas Turbines Power, vol. 106, no. 1, Jan. 1984, pp. 241-245.

7. Brown, A.; Mandjikas, B.; and Mudyiwa, J. M.: Blade Trailing Edge Heat Transfer. ASME Paper 80-GT-45, Mar. 1980.

8. Miller, R. L.: ESCORT: A Data Acquisition and Display System to Support Research Testing. NASA TM-78909, 1978.

9. Hilsenrath, J., et. al.: Tables of Thermal Properties of Gases. NBS-Circ-564, 1955.

10. Eckert, Ernst R. G.; and Drake, Robert M.: Heat and Mass Transfer. Second ed. McGraw-Hill, New York, 1959, p. 270.

11. Kline, S. J.; and McClintock, F. A.: Describing-Uncertainties in Single-Sample Experiments. Mech. Eng., vol. 75, no. 1, Jan. 1953, pp. 3-8.

TABLE I. - TEST SECTION DIMENSIONS

Configuration	X_t	X_s	Length, cm	Inlet		Exit	
				Width, cm	Height, cm	Width, cm	Height, cm
Constant height	4	2	9.58	12.7	1.27	6.35	1.27
Constant width	4	2-1	9.58	12.7	1.27	12.7	0.64
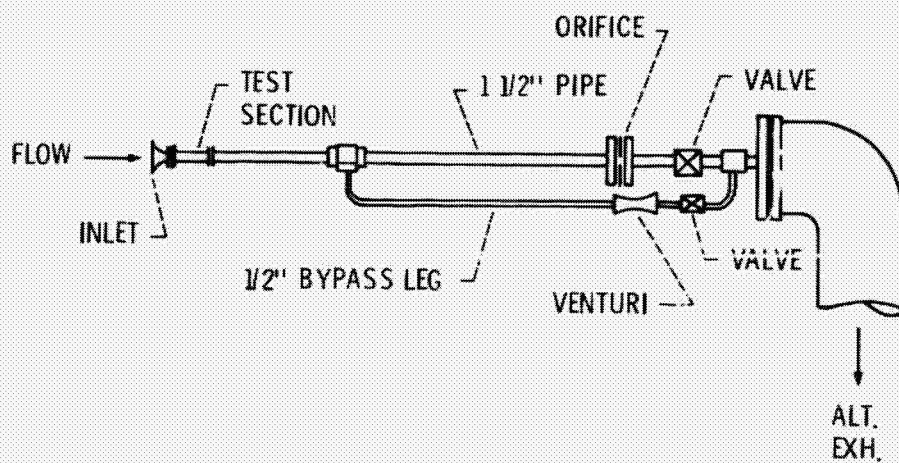
Figure 1. - Pin fin heat transfer rig.
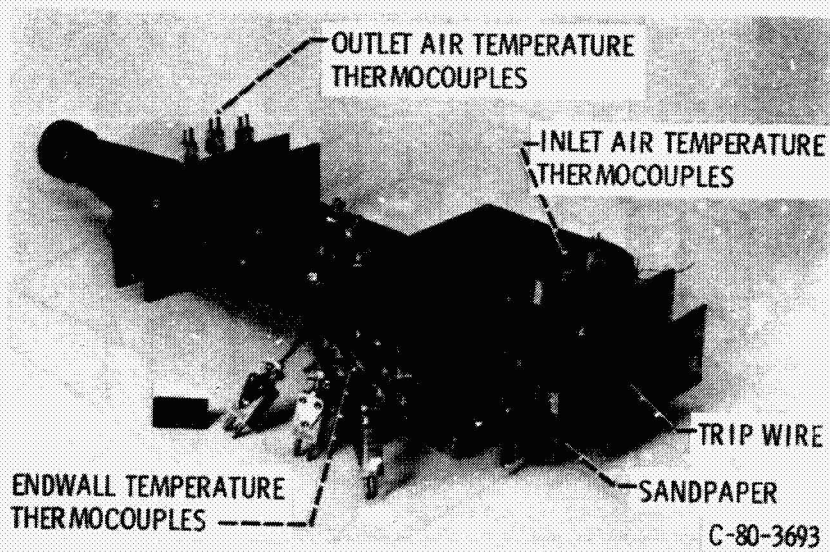
Figure 2. - Pin fin test section assembly.
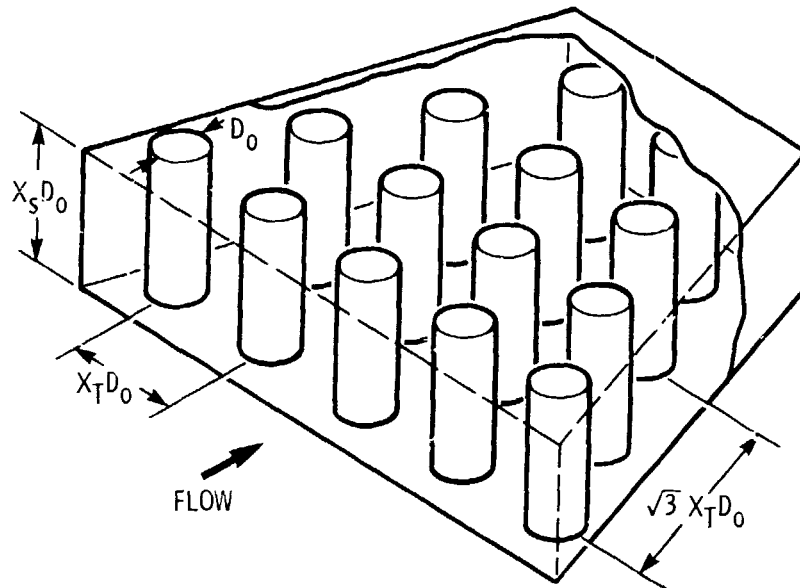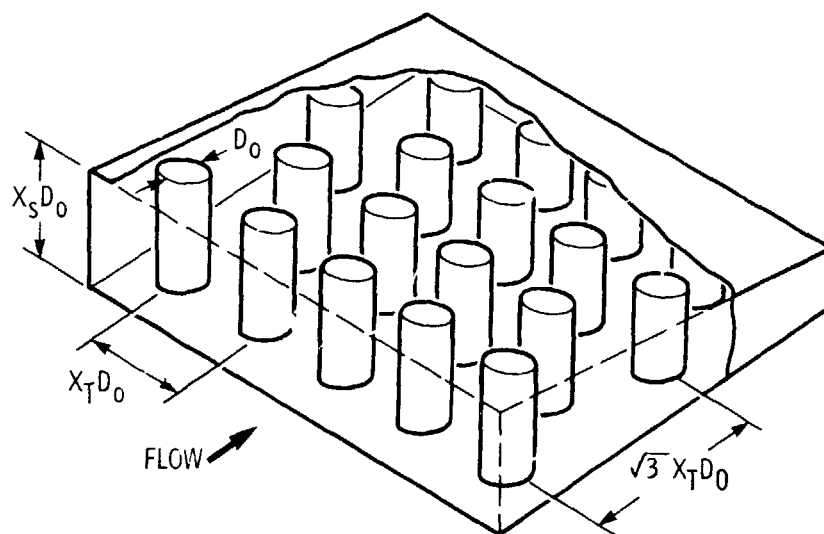
Figure 3. - Schematic of constant height test section.

Figure 4. - Schematic of constant width test section.
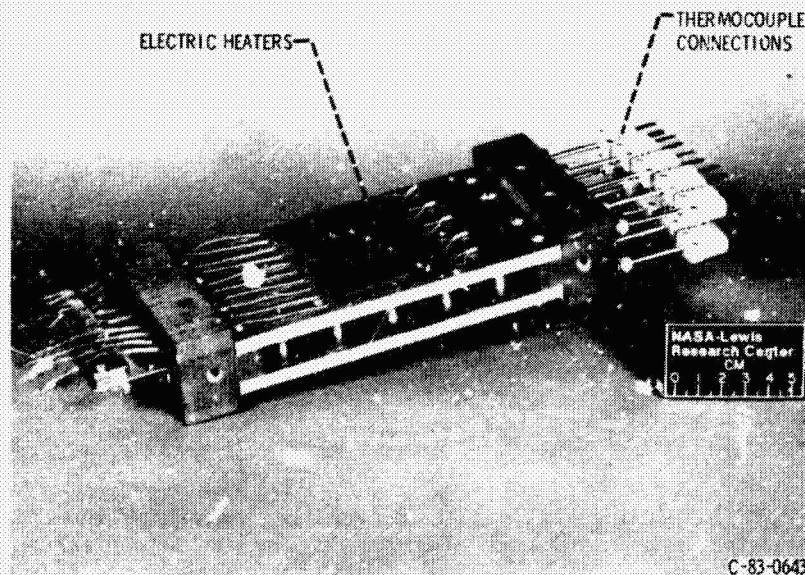
THERMOCOUPLE
CONNECTIONS

ELECTRIC HEATERS

CM NASA
0   2.5
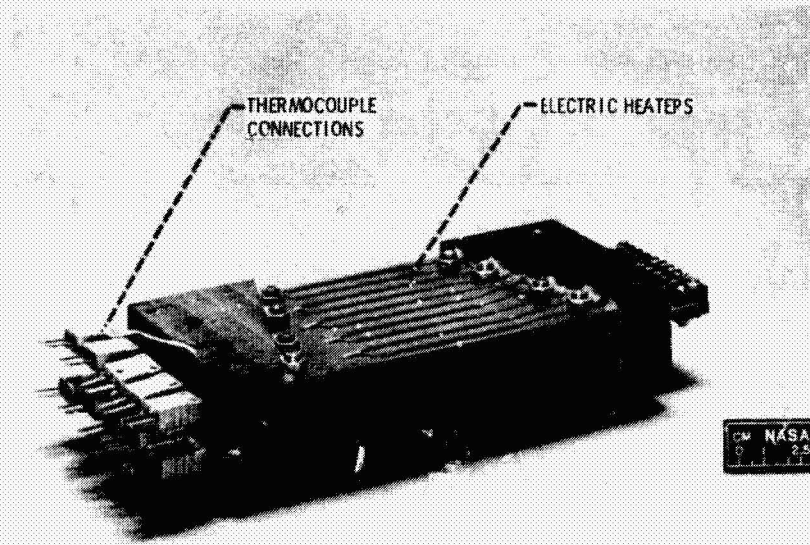
C-83-6573

Figure 5. - Constant height test section.

ELECTRIC HEATERS

THERMOCOUPLE
CONNECTIONS

NASA-Lewis
Research Center
CM
0 1 2 3 4 5

C-83-0643

Figure 6. - Constant width test section.
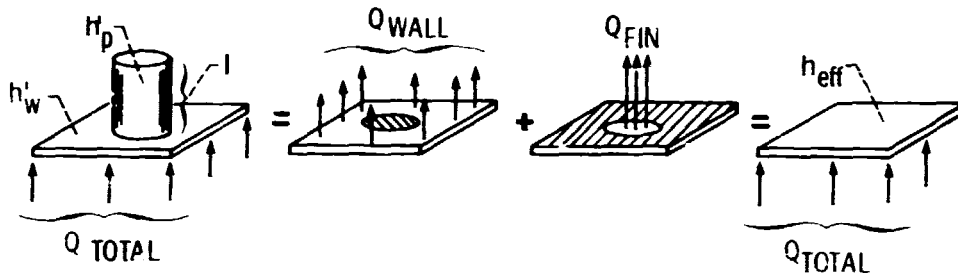
$$Q_{TOTAL} = Q_{WALL} + Q_{FIN}$$

$$Q_{TOTAL} = h'_w (A_w - A_p)(T_w - T_{aw}) + \sqrt{Ph'_p k_p A_p} \ \tanh(ml)(T_w - T_{aw})$$

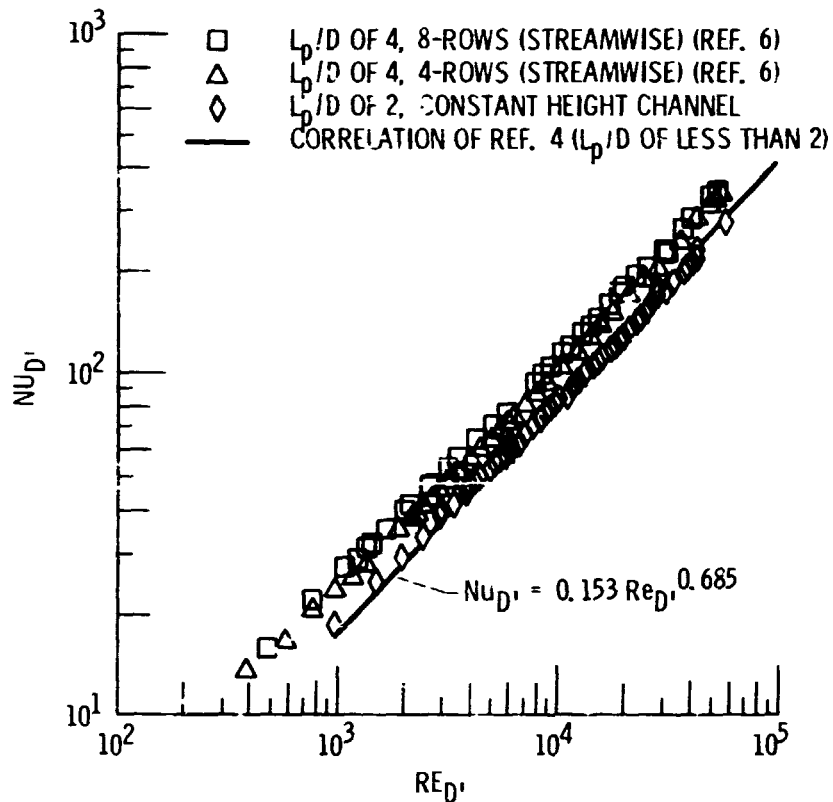$$Q_{TOTAL} = h_{eff} A_w (T_w - T_{aw})$$

Figure 7. - Theoretical model.

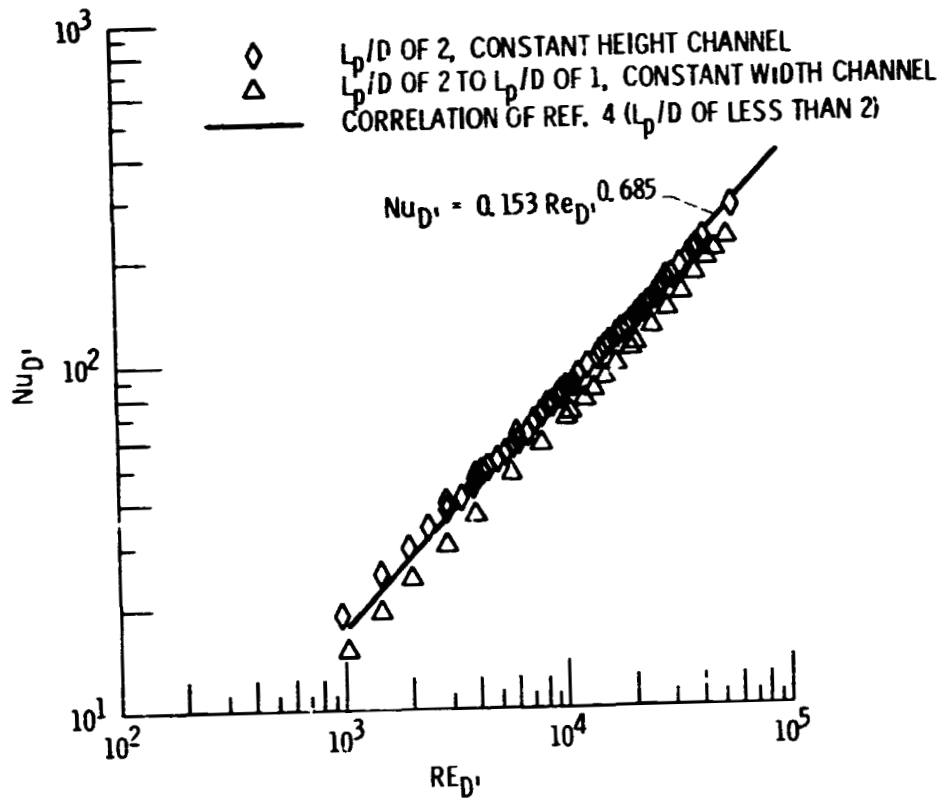Figure 8. - Constant height data plotted with results of refs. 4 and 6.

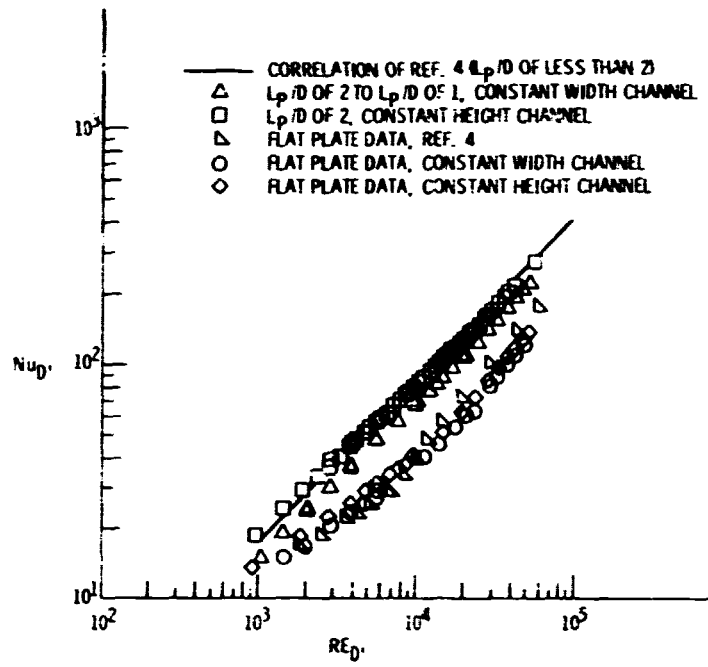Figure 9. - Current data plotted with results of ref. 4

Figure 10. - Current pin fin data plotted with current flat plate data.